



Microbial dynamics in shallow CO₂ seeps system off Panarea Island (Italy)

Amira Saidi^{1,2} · Elisa Banchi¹ · Viviana Fonti¹ · Vincenzo Manna¹ · Cinzia De Vittor¹ · Michele Giani¹ · Francesca Malfatti^{1,3} · Mauro Celussi¹

Received: 19 September 2022 / Accepted: 7 June 2023 / Published online: 24 June 2023
© The Author(s) 2023

Abstract

Shallow-water hydrothermal vents are extreme environments characterized by high temperatures, low pH, and high CO₂ concentrations; therefore, they are considered as suitable laboratories for studying the effect of global changes on marine microbes. We hypothesized a direct effect of vents on prokaryotic community structure and functioning in the Panarea Island's hydrothermal system. Sampling was conducted along a 9-station transect characterized by three active emission points. The water column was stratified with a thermocline at 25 m depth and a deep chlorophyll maximum between 50 and 100 m. Prokaryotic abundance ranged from 0.2 to 1.5 × 10⁹ cells L⁻¹, prokaryotic carbon production from 2.4 to 75.4 ng C L⁻¹ h⁻¹, and exoenzymatic activities degrading proteins, phosphorylated compounds, and polysaccharides were on the order of 4–28, 2–31 and 0.2–4.16 nM h⁻¹, respectively. While microbial abundance and production were shaped by the water column's physical structure, alkaline phosphatase and beta-glucosidase activities seemed to be enhanced by hydrothermal fluids. The 16S rRNA gene amplicon sequencing analysis identified a surface, a deep, and a vent-influenced microbial community. In terms of relative abundance members of the SAR11 group dominated the water column, alongside *Synechococcus* and *Prochlorococcus* in surface and bottom samples, respectively. Vent-influenced stations were characterized by the presence of *Thiomicrospira*, a sulfur-oxidizer chemolithoautotroph. Overall, this study provides insights on the coupling between microbial community structure and the biogeochemical cycling of nutrients in low-pH conditions (CO₂ and H₂S-based), thus addressing some of the opened questions about the response of microbes to acidification.

Keywords Hydrothermal vent · Biogeochemical cycling · Microbial abundance · DNA metabarcoding · Mediterranean · Acidification

Introduction

Marine hydrothermal systems are part of active submarine volcanic areas (Gugliandolo and Maugeri 2019). Fluids

emitted from vents are characterized by high temperatures, and high concentrations of chemicals (CO₂, H₂S, hydrocarbons, and heavy metals), thus representing extreme habitats for marine microbes, impacting the local biogeochemical cycles (Jannasch et al. 1985; Karl 1995).

Since November 2002, when a gas emission spike was detected, Panarea's hydrothermal vent system became a critical area to study for a better understanding of hydrothermal vent dynamics (Italiano and Nuccio 1991; Maugeri et al. 2009). On a biological perspective, systems like the hydrothermal field of Panarea can be used as natural laboratories for studying the effect of ocean acidification on the marine biota. In fact, the increased concentration of carbon dioxide that lowers the seawater's pH can simulate acidification both due to increased atmospheric CO₂ partial pressure (González-Delgado and Hernández 2018) and to leakages from CO₂ geological storage sites

Responsible Editor: D. K. Ngugi.

- ✉ Amira Saidi
asaidi@ogs.it
- ✉ Francesca Malfatti
fmalfatti@units.it
- ✉ Mauro Celussi
mcelussi@ogs.it

- ¹ Istituto Nazionale Di Oceanografia E Di Geofisica Sperimentale, OGS, Trieste, Italy
- ² Ca' Foscari Università Di Venezia, Venice, Italy
- ³ Università Degli Studi Di Trieste, Trieste, Italy

(e.g., Jones et al. 2015; Molari et al. 2018) with consequent solubilization in the ocean.

Several studies have investigated the impact of increased CO₂ concentration on planktonic prokaryotes under controlled and simulated conditions (Riebesell and Gattuso 2015; Boyd et al. 2018). On a general perspective, many studies have been focusing on the alteration of the organic carbon pool due to different responses of phytoplankton production to ocean acidification (e.g., Flynn et al. 2015; Bach and Taucher 2019; Taucher et al. 2021). Since organic matter is the source of C and energy for most organotrophic prokaryotes, a secondary effect on prokaryotic community structure and functioning has been hypothesized. For example, Tsiola et al. (2023) recently demonstrated that members of SAR11 can be favored over other taxa by acidified conditions, yet other studies have reported controversial results on community shifts (e.g., Liu et al. 2010 and references therein). Likewise, the effect of ocean acidification on the processing of organic matter by prokaryotes (degradation and utilization rates) has been shown to vary in different locations and trophic regimes (e.g., Sala et al. 2016; Celussi et al. 2017; Hu et al. 2021).

Utilizing a different approach, other authors have explored the possibility of exploiting the natural features of shallow hydrothermal vents to simulate future acidification scenarios (e.g., Lidbury et al. 2012; González-Delgado and Hernández 2018; Tangherlini et al. 2021). However, a disadvantage of using natural systems of volcanic origin is the presence of other associated chemicals in hydrothermal fluids such as H₂S and CH₄ (González-Delgado and Hernández 2018) that can create a unique environment for the growth of specialized microorganisms. In fact, hydrothermal vent microbes are able to use the energy and chemicals released from vents to produce organic matter through chemosynthesis (Tarasov et al. 2005). An extensive body of literature indicates that low levels of S-compounds in the emitted fluids can promote the prevalence of sulfur cycling prokaryotes in the proximity of vents (Maugeri et al. 2009; González et al. 2020; Rizzo et al. 2022; Scutтери et al. 2022). In addition to chemosynthetic microorganisms, photosynthetic bacteria have been found to play an important role in shallow hydrothermal vent systems, by converting CO₂ to organic matter contributing significantly to primary production (Gomez-Saez et al. 2016).

Studies at the shallow hydrothermal system of the Panarea Island, showed the presence of photosynthetic and chemolithotrophic primary producers both in seawater and sediments (e.g., Manini et al. 2008; Maugeri et al. 2009, 2010; Karuza et al. 2012; Lentini et al. 2014; Bortoluzzi et al. 2017; Tangherlini et al. 2021; Rizzo et al. 2022 and references therein), highlighting fine-tuned adaptation and survival strategies in this peculiar environment.

Within this framework, we tested whether the vents (i.e., lower pH) influenced the composition of microbial communities and, for the first time in this environment, we combined the molecular-based data with the organic matter pool processing (i.e., degradation and utilization) in the water column.

Materials and methods

Sampling design

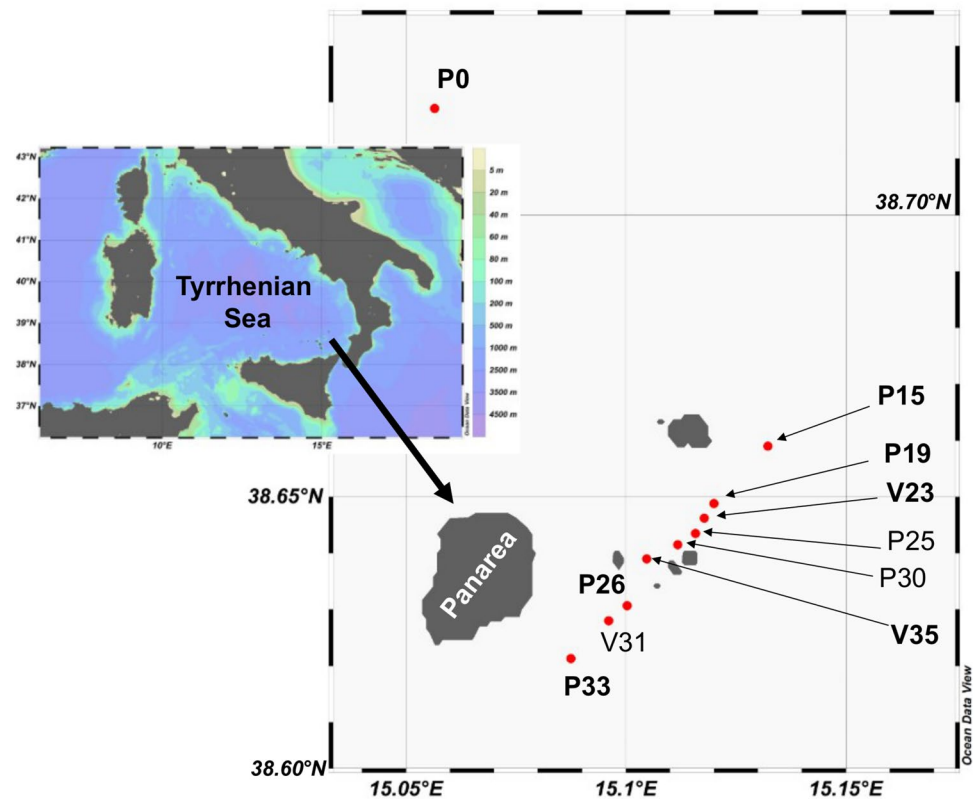
Sampling was carried out between 28th and 31st July 2011 in the Panarea Island area (Fig. 1; Supplementary Table S1) along a 9-station transect. One extra station located north of the vent field was sampled as a reference (i.e., no vent-influenced). At each station, temperature, salinity, oxygen, and pH vertical profiles were registered using a CTD SBE9 Seabird. Seawater was collected with 10 L Niskin bottles for determining pH, the concentrations of chlorophyll *a*, macronutrients, dissolved inorganic carbon, particulate organic carbon, and nitrogen concentrations, as well as prokaryotic abundance, the rates of heterotrophic carbon production and extracellular enzymatic activities, and to depict the prokaryotic community structure by 16S rRNA gene amplicon sequencing (at seven stations). Samples were collected in the surface (~2 m depth, named *surface*) and bottom layers (collected a few meters above the seafloor, or at a depth ~45 m at the stations deeper than 100 m—stations P0 and P15-, named *bottom*). Additional intermediate sampling depths were selected according to the CTD profiles of temperature, salinity and pH (Supplementary Table S1). Within the transect, three active vents were detected (stations V23, V35, and V31).

Chemical and microbiological analyses

Seawater samples for determining chlorophyll *a* concentration were filtered through Whatman GF/F glass-fiber filters (0.7 µm nominal pore size, 47 mm diameter) and immediately frozen (−20 °C) until analysis. Pigments were extracted from the grinded filters overnight in the dark at 4 °C with 90% acetone and determined fluorometrically according to Lorenzen and Jeffrey (1980). The readings of the extracts were performed before and after acidification with two drops of HCl 1 N using a JASCO FP 6500 spectrofluorometer (450 nm excitation and 665 nm emission wavelengths). Calibration curves were prepared using pure chlorophyll *a* standard from spinach (Sigma-Aldrich).

Water samples for pH measurement (pH_T) were collected directly into quartz cuvettes with a 10 cm path length, overflowing with twice the cuvette volume and no head space. pH analyses were carried out immediately onboard against

Fig. 1 Sampling stations in the Panarea Island area, Tyrrhenian Sea. Bold fonts indicate stations where 16S rRNA gene amplicon sequencing analysis was performed. The color scale indicates the bathymetry in meters. The map was created with Ocean Data View (Schlitzer 2018)



MilliQ water in a Varian Cary 50 single beam spectrophotometer with thermostatted cylindrical cuvette holders. A circulating bath was used to maintain the temperature at 25.0 °C. The temperature in the cuvette was controlled with a PT100 temperature sensor (precision: 0.01 °C, GMH 3750). The indicator m-cresol violet was added to the cuvette using a micropipette. The SOP6b ver 3.01 (Dickson et al. 2007) method was followed. The in situ pH, expressed on the total scale, was calculated on the basis of the in situ temperature and salinity measured by the CTD probe.

Samples for dissolved inorganic carbon concentration (DIC) analyses were collected in HCl-washed glass vials minimizing gas exchange with the atmosphere, treated with a mercuric chloride solution (0.04% by volume of a saturated aqueous solution) in order to prevent biological activity, sealed with a Teflon cap, and stored refrigerated until analyses. DIC was determined using a Shimadzu TOC-V CSH analyzer. Samples were injected into the instrument port and directly acidified with H₃PO₄ (25%). Phosphoric acidification generated CO₂ that was carried to a nondispersive infrared detector (NDIR). The analysis showed a variation coefficient <2%. The reproducibility of the method was between 1.5 and 3%.

Seawater samples for dissolved inorganic nutrient analysis (NH₄⁺, NO₂⁻, NO₃⁻ and PO₄³⁻) were prefiltered on 0.7 μm pore size glass-fiber filters (Whatman GF/F) and then immediately frozen. Samples were analyzed at room temperature

on a continuous flow autoanalyzer (Bran + Luebbe, Norderstedt, Germany), according to Koroleff and Grasshof (1983). The efficiency of the system was checked before and after sample analyses by doing replicates of internal standards. Dissolved inorganic nitrogen (DIN) was calculated as the sum of NH₄⁺, NO₂⁻ and NO₃⁻.

For determining particulate organic carbon and nitrogen concentration, seawater samples were filtered through pre-combusted 25 mm Whatman GF/F filters. The filters were frozen at -20 °C. Before the analysis, the filters were treated with 1 N HCl to remove carbonates (Lorrain et al. 2003) and then oven-dried at 60 °C for 1 h. A CHNO-S elemental analyzer Costech mod. ECS 4010 was used to measure carbon and nitrogen according to Pella and Colombo (1973) and Sharp (1974). The analysis was performed by combustion of the sample in oxygen excess at 980 °C with Cr₂O₃ catalyst and reduction in a column filled with reduced copper wires at 650 °C. CO₂ and N₂ were separated in a HayeSepQ divinylbenzene packed column at 70 °C, using helium as carrier gas, and measured with a thermal conductivity detector. Filter blanks were analyzed and subtracted. The C and N sample concentrations were expressed as μg C L⁻¹ and μg N L⁻¹, respectively.

Samples for prokaryotic abundance (heterotrophs-HP, *Synechococcus*-SYN) were fixed with 0.22 μm filtered buffered formaldehyde solution (2% final concentration) and flash frozen in liquid nitrogen according to Patel et al.

(2007). Samples were processed according to Noble and Fuhrman (1998) within 1 month. Samples (0.5–1.5 mL) were filtered onto 0.02 μm pore-size Al_2O_3 inorganic membrane filters (Anodisc, Whatman), then stained with SYBR Green I 50 \times (final concentration), mounted on a glass slide with antifade solution (50% glycerol, 49% PBS and 1% ascorbic acid) and stored at -20°C . The enumeration was done by epifluorescence microscopy (Olympus BX 60 F5) at 1000 \times magnification under a blue (BP 450–480 nm, BA 515 nm) and a green (BP 480–550 nm, BA 590 nm) (Waterbury et al. 1979) filters set for HP and SYN, respectively. A minimum of 300 cells was counted for each filter in at least 20 randomly selected fields. All samples were run in three replicates and values represent their mean \pm a standard deviation <10%.

Prokaryotic carbon production (PCP) was measured by the incorporation of ^3H -leucine (Leu) (Kirchman et al. 1985). Triplicate aliquots (1.7 mL) and two controls killed by the addition of 90 μL 100% trichloroacetic acid (TCA) were amended with a 20 nmol L^{-1} radiotracer and incubated at in situ temperature in the dark. Incubations were stopped with TCA (5% final concentration) after 1 h. The extraction with 5% TCA and 80% ethanol was carried out using the microcentrifugation method (Smith and Azam 1992). Activity in the samples was determined by a β -counter (TRI-CARB 2900 TR Liquid Scintillation Analyzer) after the addition of 1 mL scintillation cocktail (Ultima GoldTM MV; Packard). Carbon biomass production was estimated using the conversion factor 3.1 kg C mol^{-1} Leu assuming a twofold isotope dilution (Simon and Azam 1989). The standard deviation among replicates was <10% of the average.

Extracellular enzymatic activities were measured following the fluorogenic substrate analogues method (Hoppe 1993) using 7-amino-4-methyl-coumarin (AMC) and 4-methyl-umbelliferone (MUF). Leucine aminopeptidase, β -glucosidase and alkaline phosphatase were assayed as the hydrolysis rate of leucine-AMC, MUF- β -D-glucoside, and MUF-phosphate, respectively. Enzyme activities were expressed in terms of the rate of MUF or AMC production. After evaluation of the saturating concentrations, hydrolysis rates were measured by incubating 2.5 mL subsamples with 200 $\mu\text{mol L}^{-1}$ MUF- β -D-glucoside, leucine-AMC, and 50 $\mu\text{mol L}^{-1}$ MUF-phosphate for 1 h in the dark at in situ temperature. The fluorescence increase due to AMC and MUF hydrolyzed from the model substrates was measured using a Shimadzu RF-1501 spectrofluorometer (AMC = 380 nm excitation and 440 nm emission; MUF = 365 nm excitation and 455 nm emission). Triplicate blanks without fluorogenic substrate were used to determine the natural fluorescence increase in the samples not attributable to the tested enzymes. Filtered seawater (0.2 μm) collected at every environmental pH was used to produce calibration curves (in three replicates) by adding 5 $\mu\text{mol L}^{-1}$

standard solutions of MUF and AMC. All samples were run in three replicates and values represent their mean \pm a standard deviation <10%.

DNA extraction, amplicon library preparation, and sequencing

For each sample, 1 L of seawater was filtered onto a 0.22 μm Supor membrane on a sterile filtration column, filters were flash frozen in liquid nitrogen and once in the laboratory, stored at -20°C . DNA was extracted using the Dneasy Power Water kit (Qiagen) following the manufacturer's instructions. Extracted DNA was quantified by a Qubit Fluorometer (Thermo Fisher Scientific) and stored at -80°C until further analysis. DNA was PCR amplified by using the primer pair 515F-Y (5'-GTGYCAGCMGCCGCGGTAA-3') and 926R (5'-CCGYCAATTYMTTTRAGTTT-3'), which encompass the V4 and V5 hypervariable loops of 16S rRNA genes (Parada et al. 2016). Libraries were prepared following the 16S Metagenomic Sequencing Library Preparation protocol (Illumina 2013) and run on an Illumina NovaSeq System for a read length of 2×250 bp at the genetic and epigenetic ARGO Open Lab Platform, Area Science Park, Trieste, Italy.

Bioinformatic pipeline

Bioinformatic analyses were carried out with QIIME2 2020.6 (Bolyen et al. 2019). Given the high number of reads produced by the NovaSeq (i.e., 46,985,351) we applied a 30% subsampling threshold prior running the bioinformatic pipeline in order to decrease the computational demand. The inspection of the rarefaction curves (Supplementary Figure S1) ensured that the sequencing effort was more than enough to assess the microbial diversity. Based on visual inspection of quality profiles, forward and reverse raw sequences were then trimmed at 240 bp and 220 bp, respectively. Reads were then filtered, denoised, and used to infer amplicon sequence variants (ASVs) using the dada2 qiime2 plugin (Callahan et al. 2016). Taxonomy was assigned using the sklearn I Bayes taxonomy classifier (Bokulich et al. 2018) against the Silva 138.1 99% reference database (Quast et al. 2013). Reads belonging to Eukarya, mitochondria, chloroplasts, and ASVs with frequency <2 (singletons) were removed.

Statistical analysis

We used the R environment (v. 3.6.2, R Core Team 2019) for statistical analyses and data visualization. A principal component analysis (PCA) was performed using all the physical, chemical and microbiological data by using the *FactoMineR* 4.2.2 package in R. Because the variables used had different units, we scaled them to mean = 0 and variance = 1 before

performing the analysis. The PCA results were extracted and visualized using the *factoextra* 4.2.2 R package (Le et al. 2008).

Microbial diversity was explored and visualized with the packages *phyloseq* 3.16 (McMurdie and Holmes 2012) and *ggplot2* 3.3.6 (Wickham 2016).

To further investigate the environmental drivers of the communities, we used a distance-based redundancy analysis (dbRDA) based on a Bray–Curtis distance matrix calculated on relative abundances using the *capscale* function in the R package *vegan* 2.6-2 (Oksanen et al. 2019). The analysis was applied only to *surface* and *bottom* data, i.e., where samples for DNA metabarcoding were collected. The environmental variables salinity, depth, pH, Chla, dissolved oxygen, DIC, POC, PN, temperature, and nutrients were first checked for collinearity inspecting pairwise scatterplots and correlation coefficients, according to the approach proposed by Zuur et al. (2010). The final set of environmental variables used in the dbRDA was then selected taking into account the multicollinearity and their ecological relevance. The significance of the selected dbRDA model was assessed by hypothesis testing (i.e., ANOVA).

Results

Water column features

The area was characterized by a thermocline between 25 and 50 m depth separating warmer surface waters (>25.6 °C) from colder subsurface ones (14.3 to 16.1 °C below 50 m)

(Fig. 2a). High salinity (>37.9) surface and deep layers were separated by a lower salinity (37.5–37.8) layer between 20 and 70 m depth (Fig. 2b). CTD-derived chlorophyll *a* concentration profiles (Fig. 2c) highlighted the presence of a deep chlorophyll maximum from 40 to approximately 150 m (data not shown), displaying the maximum values around 70–90 m depth. These features affected the dissolved oxygen concentration, whose spatial distribution showed lower levels (195–200 $\mu\text{mol L}^{-1}$) in surface waters in the upper 20 m, below which an oxygen-rich layer was present in correspondence of lower salinity and higher phytoplankton biomass, reaching the highest values of 250–260 $\mu\text{mol L}^{-1}$ between 35 and 55 m.

The higher phytoplankton biomass in deep waters was also confirmed by the analyses of discrete samples for chlorophyll *a* concentration that showed the highest values (0.3 $\mu\text{g L}^{-1}$) below 70 m (Fig. 3a). Along the transect, a drop in pH_T (Fig. 3b) was detected in the vent-influenced stations V31, V35, and V23. The minimum value was 7.31, measured at 20 m depth at station V35. It is also noteworthy that the acidification effect of the vent plume reached the surface ($\text{pH}_T = 7.62$) at this station, likely due to the shallow depth. Because of dilution and mixing of the vent fluid with seawater, the pH_T at the third vent-associated station (V31) increased to ambient seawater levels (8.00) at mid-depth (54 m).

Dissolved inorganic carbon (DIC, Fig. 3c) concentrations were higher (up to 39.76 mg L^{-1}) in bottom waters, especially in the vent-associated station V35. Station P19 had the lowest DIC concentration in the intermediate layer (30.11 mg L^{-1}), along with maximum pH values. The

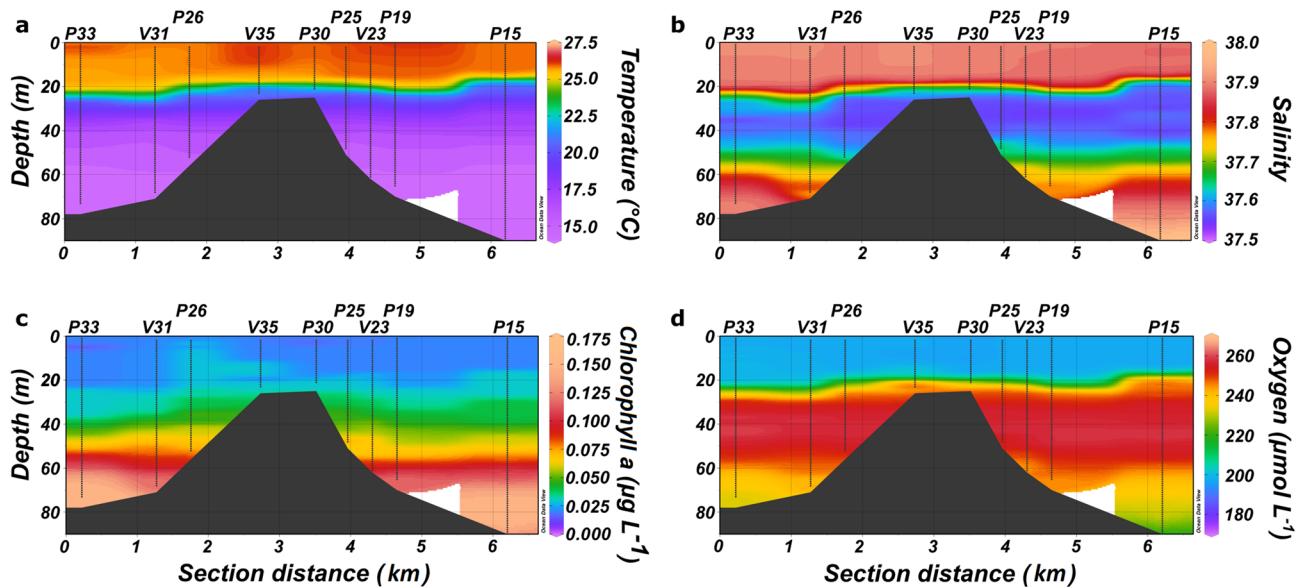


Fig. 2 CTD-derived data of **a** temperature, **b** salinity, **c** chlorophyll *a*, and **d** dissolved oxygen concentrations along the transect. The contour plots were created with Ocean Data View (Schlitzer 2018)

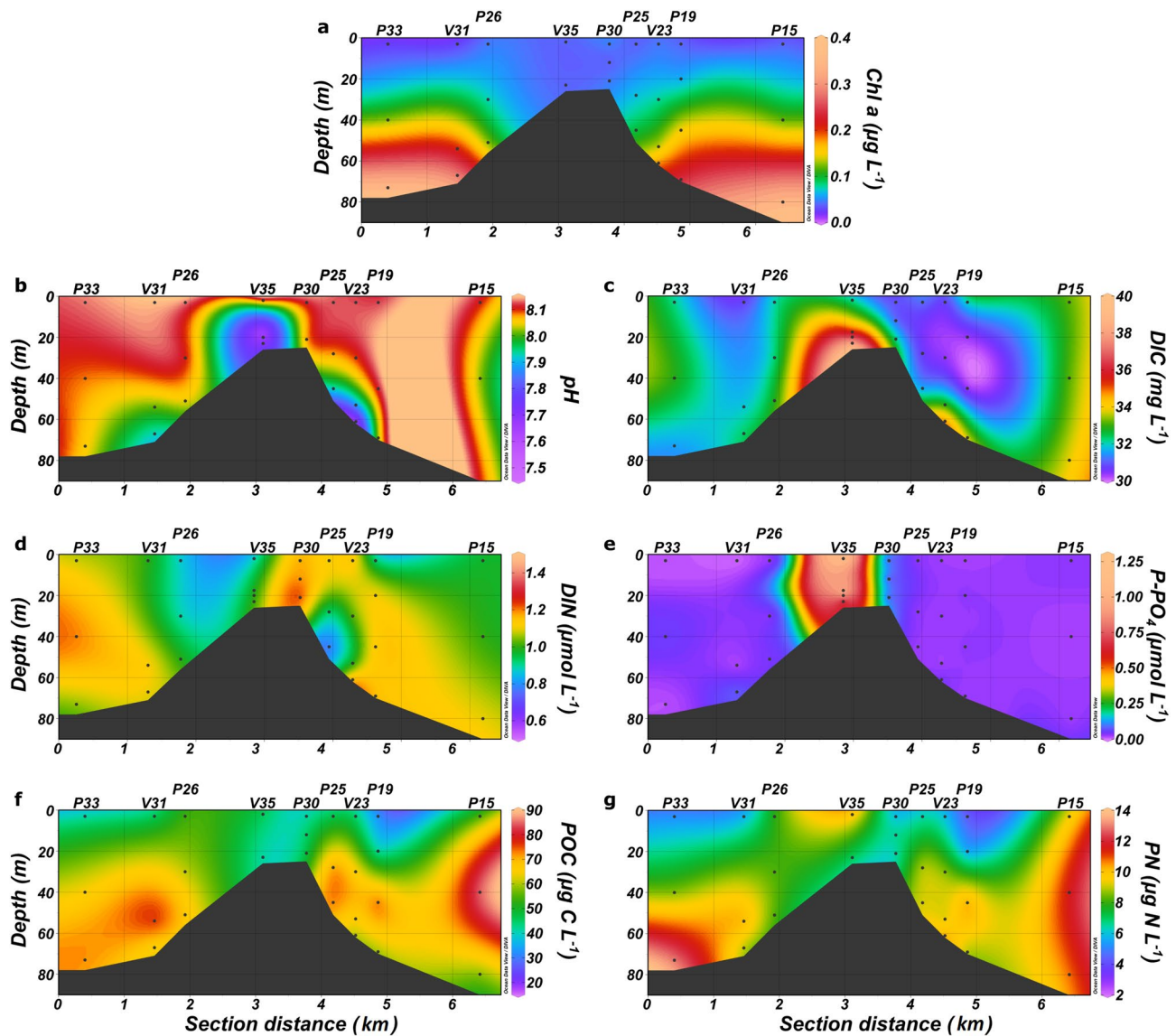


Fig. 3 Water column environmental features: **a** chlorophyll *a* (Chl *a*, extracted from filters), **b** pH_T, **c** dissolved inorganic carbon (DIC), **d** dissolved inorganic nitrogen (DIN), **e** phosphate (P-PO₄), **f** particulate

organic carbon (POC), **g** particulate nitrogen (PN). The contour plots were created with Ocean Data View (Schlitzer 2018)

concentration of inorganic nutrients (Fig. 3d, e) indicated a general oligotrophic condition. Dissolved inorganic nitrogen concentrations were highly heterogeneous along the transect (DIN, Fig. 3d) ranging from 0.7 to 2.4 $\mu\text{mol L}^{-1}$. Phosphate concentrations were in general between 0.01 and 0.07 $\mu\text{mol L}^{-1}$, but at station V35, in proximity to one of the vents, the highest value of 1.28 $\mu\text{mol L}^{-1}$ was measured both at the surface and at 20 m depth. Particulate nitrogen (PN, Fig. 3f) and particulate organic carbon (POC, Fig. 3g) showed comparable distributions along the transect with higher values in the bottom layer than at the surface. The highest values of PN and POC were measured at station P15. POC concentration was higher than PN with a range

of 30–80 $\mu\text{g C L}^{-1}$ vs 4–14 $\mu\text{g N L}^{-1}$, respectively. All data generated at station P0, not represented in the contour plots, are reported in Supplementary Table S2.

Microbial dynamics in water column

HP (Fig. 4a) ranged from 0.2 to 1.5×10^9 cells L^{-1} , with the maximum value recorded at station P25 and the lowest abundance at station P15. *Synechococcus* was more abundant at the surface (Fig. 4b), ranging from 0.3 to 2.1×10^7 cells L^{-1} .

To assess the vent effect on microbial organic matter degradation, we measured the activity (Fig. 5) of leucine-aminopeptidase (AMA), alkaline phosphatase (APA), and

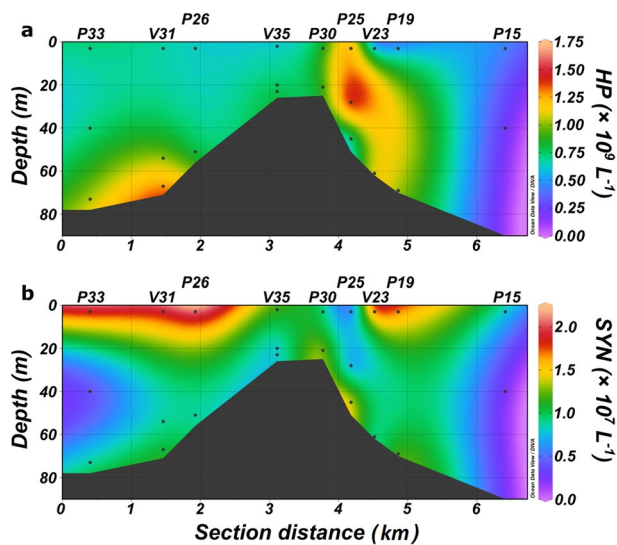


Fig. 4 Abundance of **a** heterotrophic prokaryotes (HP) and **b** *Synecococcus* (SYN) along the transect. The contour plots were created with Ocean Data View (Schlitzer 2018)

β -glucosidase (BGLU). Leucine aminopeptidase (Fig. 5a) rates were the highest at the surface at stations P19 and P25. At the vent stations V35, V23, and V31, AMA showed intermediate values at the bottom (15 nM h^{-1} , Fig. 5a). Alkaline phosphatase (Fig. 5b) rates were generally low (<10 nM h^{-1}) in the area, with a spike (20 nM h^{-1}) of activity in venting station V35 where the highest phosphate and DIC concentrations were measured. A similar pattern was evident for

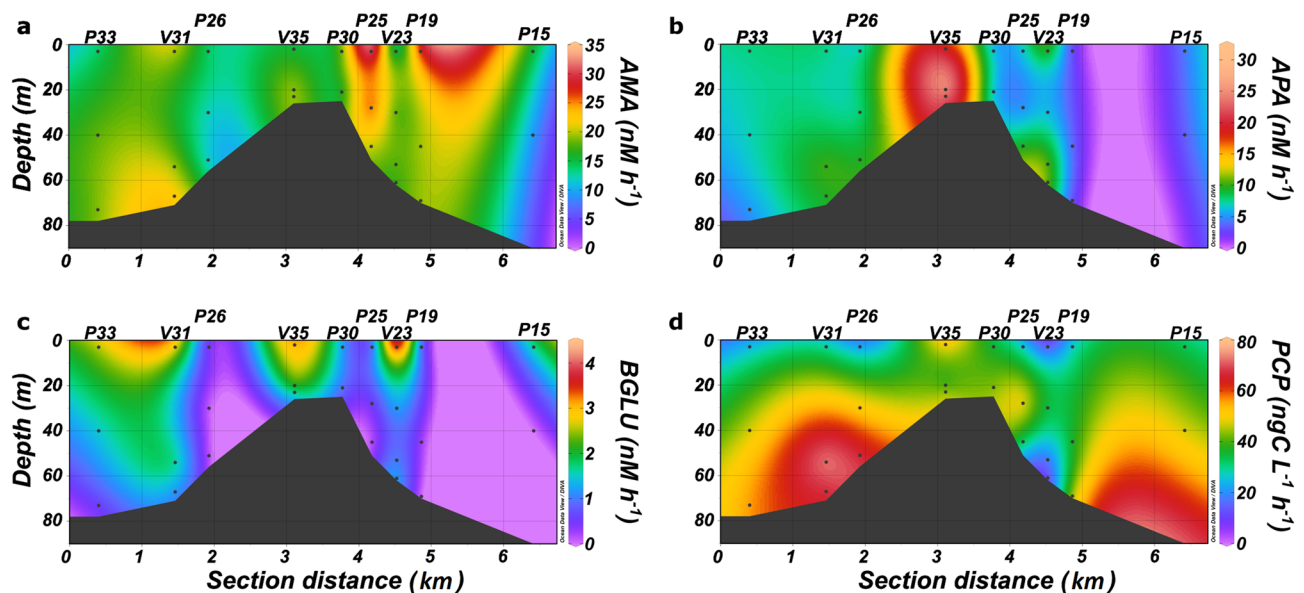


Fig. 5 Extracellular enzymatic activities and prokaryotic carbon production along the transect: **a** leucine-aminopeptidase (AMA), **b** alkaline phosphatase (APA), **c** beta-glucosidase (BGLU), **d** prokaryotic

BGLU (Fig. 5c), with faster rates (>3 nM h^{-1}) in the surface layer of vent-affected stations (V31, V35, and V23).

Prokaryotic carbon production rates (PCP, Fig. 5d) mirrored the chlorophyll *a* concentration with higher values in the bottom samples collected in the southern sector of the transect (Max = 75.4 $\text{ng C L}^{-1} \text{h}^{-1}$; Fig. 5d).

Relationship between environmental and biological variables

The principal component analysis (Fig. 6) of physical, chemical, and microbiological data showed a separation of samples according to depth (and the depth-related variables temperature, Chl*a*, DO, POC, PN and PCP) along the first principal component, accounting for 37.1% of the total variance. APA, DIC, Phosphate, and pH were correlated with PC2 (Fig. 6) and explained 19.4% of the total variance.

Overall, the variables correlated with PC1 were affected by the physical structure of the water column, whereas the variables correlated with PC2 were affected by the vent emissions.

Prokaryotic diversity and community composition

16S rRNA gene analysis was performed at six stations along the transect and at the reference station P0 (Supplementary Table S1).

The relative abundance of the top 15 genera accounted for ~75% and ~66% of all reads in surface and bottom samples, respectively (Fig. 7). At the surface, the prokaryotic

carbon production (PCP). The contour plots were created with Ocean Data View (Schlitzer 2018)

Fig. 6 Principal component analysis (PCA) biplot of the physical, chemical and microbiological variables. *SYN* *Synechococcus*, *HP* heterotrophic prokaryotes, *AMA* aminopeptidase activity, *BGLU* beta-glucosidase activity, *APA* alkaline phosphatase activity, *PCP* prokaryotic carbon production, *CHLa* chlorophyll *a*, *POC* particulate organic carbon, *PN* particulate nitrogen, *Temp* temperature, *DO* dissolved oxygen, *DIN* dissolved inorganic nitrogen, *PO₄* phosphate, *DIC* dissolved inorganic carbon. Cold color gradient indicates station depth (i.e., baby blue: 1–3 m, blue 20–45 m, navy blue 50–75 m); circles indicate non-venting stations and triangles indicate venting stations

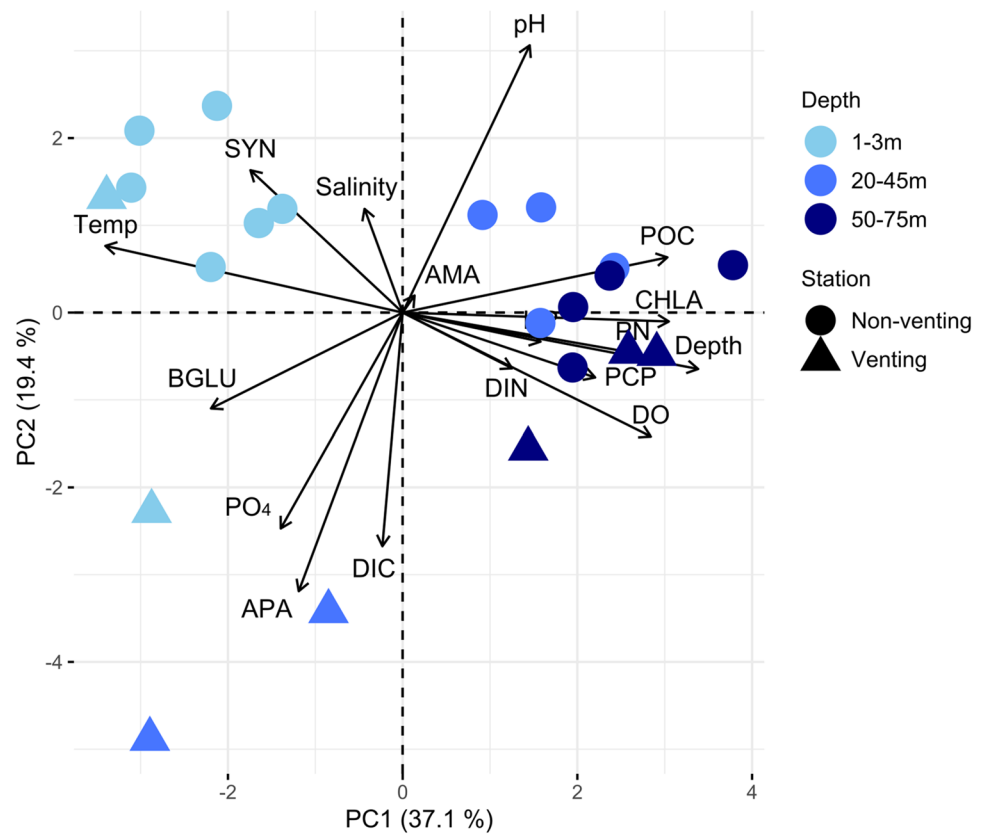
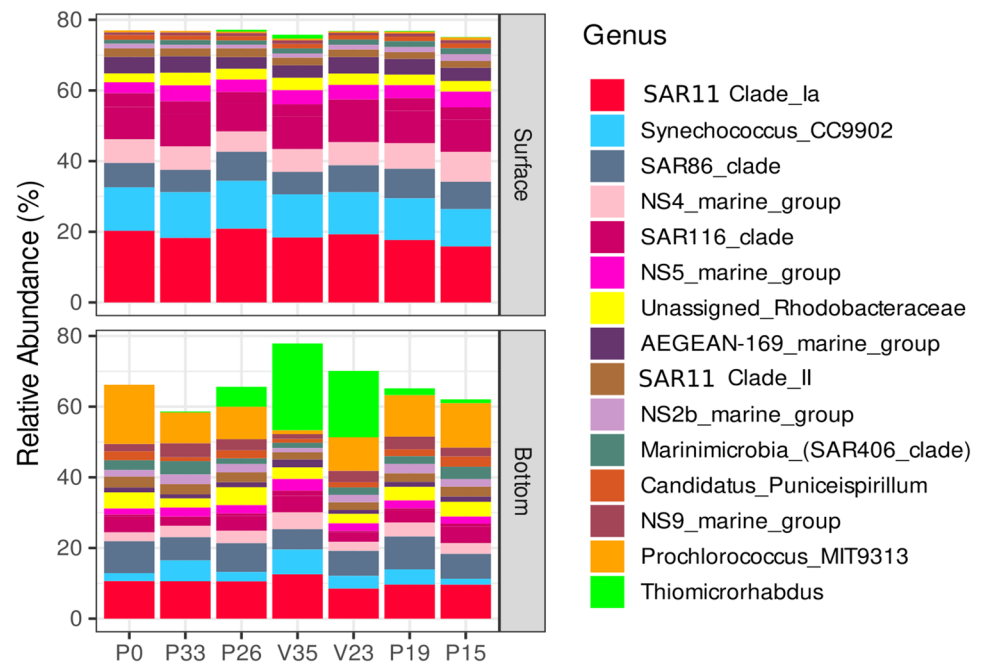


Fig. 7 Relative abundance of the top 15 genera in the seven sampling sites selected for 16S rRNA gene sequencing along the transect at different depths (surface and bottom)



assemblage was dominated by SAR11 clade Ia, SAR116 and *Synechococcus* (average relative abundance = 18.7%, 12.4% and 12.2%, respectively). At the bottom, the highest relative abundances were attributed to SAR11 clade

Ia, *Prochlorococcus* and *Thiomicrohabdus* (on average 10.3%, 9.9% and 7.6% respectively), *Thiomicrohabdus*, a sulfur oxidizer member of the Gammaproteobacteria was predominant especially at the vent-associated stations with

the highest relative abundance in V35 (24.53%) followed by station V23 (18.8%). Overall, the prokaryotic community structure of the surface differed from the bottom one, where the presence of sulfur oxidizers was typical of vent-affected stations.

The environmental data exploration highlighted collinearity between the variable depth and Chl_a, PN, POC, temperature, DO, and between DIC and pH. Therefore, the dbRDA analysis was performed using the variables depth, DIC, DIN and PO₄ (Fig. 8). The ANOVA on the dbRDA model highlighted depth (df: 1, SSE: 1.73810, F: 52.9201, $p < 0.001$) and DIC (df: 1, SSE: 0.12638, F: 3.8479, $p < 0.05$) as the main drivers shaping the community structure. In fact, also in this case the samples followed a main gradient (along RDA1) related to depth and depth-connected drivers with vent-influences samples further segregating from the other *bottom* samples (RDA2).

Discussion

Effect of vents on environmental features and microbial dynamics

Investigating the functioning of microbial communities in shallow hydrothermal vents is important to understand how

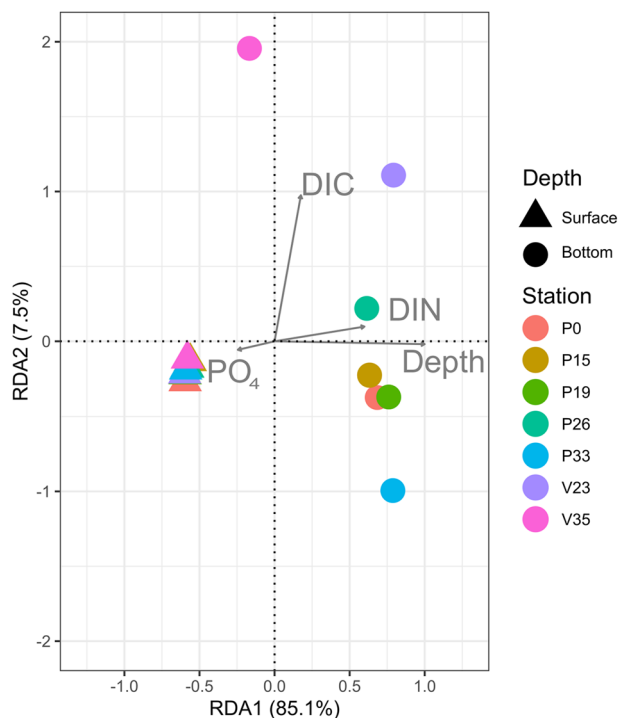


Fig. 8 Distance-based redundancy analysis (dbRDA) based on Bray-Curtis dissimilarity in community composition. *DIC* dissolved inorganic carbon, *DIN* dissolved inorganic nitrogen

microbes respond to the rapid changes in nutrient availability, pH, electron donors and in general to the chemistry of such environments. The results are discussed in the light of shallow hydrothermal vent systems and ocean acidification literature, as the main vent feature we detected at vent-affected stations was an increase in DIC (Rizzo et al. 2022 and references therein). The resulting pH variations could impact microbial responses in terms of metabolic activities and microbial community structure and diversity.

In the study area (Panarea Island), deep-origin CO₂ leaks from the sea bottom into the water column (Esposito et al. 2006). The composition of the gas is stable, with 96.6–98.6% of CO₂ and 1.2–2.2% of H₂S (Caliro et al. 2004). Thus, the vents in Panarea, as in other natural vent systems, have an impact on the chemistry of the water column, mostly affecting its pH (Dittmar and Koch 2006; Lang et al. 2006; Walker et al. 2008; Bennett et al. 2011; Gomez-Saez et al. 2016). Our results showed a drop in pH at the vent stations (V35, V23 and V31) due to elevated DIC concentrations. In addition, the area was characterized by low nutrient and chlorophyll concentrations, typical of oligotrophic Mediterranean waters (Bergamin et al. 2019). Only phosphate concentration showed a remarkable increase in the vent station V35, probably due to the turbulence induced by the seepage of gas bubbles that transported the phosphate-enriched interstitial water upwards (Molari et al. 2018). Chl_a, POC, and PON concentrations did not show evident differences among the venting and non-venting stations, as previously shown (Acosta Pomar and Giuffrè 1996).

Moreover, the thermocline formed a two-layered euphotic zone with the upper layer being characterized by higher temperature and the lower one characterized by higher Chl_a concentration (i.e., a deep chlorophyll maximum, DCM). In such a system, the thermocline had an important effect on structuring the environmental and biological parameters. For example, both prokaryotic abundance and PCP rates were higher in the DCM, thus highlighting the tight coupling between carbon fixation and prokaryotic carbon production processes (Longhurst and Harrison 1989). Furthermore, Chl_a and POC (and PN) were positively correlated (Spearman's $\rho = 0.71$, $df = 22$, $p < 0.001$), thus reflecting the increase of phytoplankton carbon biomass in the DCM (Macias et al. 2019). In contrast, APA and BGLU rates were more affected by the presence of the vent rather than by the vertical structure of the water column (Figs 5, 6).

We did not find any apparent effect of the vent on prokaryotic abundance and production. Many ocean acidification studies found that prokaryotic biomass was weakly influenced by acidification either increasing or decreasing in cell abundance (Grossart et al. 2006; Allgaier et al. 2008) although its photoautotrophic fraction (Cyanobacteria) may benefit from additional CO₂ (Hutchins et al. 2007) in fueling photosynthesis.

Prokaryotic production has been found to be either stimulated (Grossart et al. 2006), inhibited (Coffin et al. 2004), or unaffected (Allgaier et al. 2008), during ocean acidification mesocosm experiments. In our study, we did not observe any increase or decrease in prokaryotic production associated with the vent, yet a dependence of organic matter utilization on phytoplankton biomass was evidenced (Spearman's ρ between PCP and Chl a = 0.51, $df = 22$, $p = 0.05$). The relationship between environmental factors and the extracellular enzymatic activities in extreme environments, including hydrothermal vent systems, has not been adequately explored (Jacobson Meyers et al. 2014). It is known that enzyme activity depends on several conditions, such as pH, temperature, catalyst availability, concentration and structure of substrates (Fukuda et al. 2000; Pomeroy and Wiebe 2001; Arnosti 2011; Celussi et al. 2017). The vent effect was detected in terms of enhanced hydrolysis rates of alkaline phosphatase and beta-glucosidase extracellular activities (Fig. 5). The faster alkaline phosphatase rates detected in our study are most likely to be caused by P-rich compounds ejected by the vents (Molari et al. 2018). On the contrary higher beta-glucosidase activity values at the lowest pH are possibly related to high DIC concentration, as previously observed in a mesocosms experiment in the Mediterranean Sea (Celussi et al. 2017). pH plays an important role in determining the redox state of metal cofactor, the stability of enzymes and their performance, the organic matter substrate and structure, ultimately affecting the measured exoenzymatic rates (Gottschalk 1979). However, the direct effect remains difficult to assess because it is hard to separate the effect of hydrogen ion concentrations from other synchronizing factors, such as temperature, nutrient concentration, or other anthropogenic influences (Piontek et al. 2010, 2013). Our results showed that vents had no clear effect on AMA (Fig. 5), in contrast with the studies of Yamada and Suzumura (2010), and Grossart et al. (2006), where protease rates were found to be highly sensitive to acidification conditions, either suppressed or enhanced by decreasing pH. However, when comparing the results of this study with literature findings it has to be taken into account that most acidification studies are conducted using artificial CO $_2$ enrichments, often involving microbial communities not adapted to chronic exposure to low pH conditions.

In order to deepen our understanding of the consequences of ocean acidification by atmospheric CO $_2$ dissolution and by hydrothermal fluid enrichment, it will be important to examine specifically the influence of chemical processes on the activation and regulations of genes involved in extracellular enzymatic activities as well as in membrane transporters responsible for organic matter utilization.

Prokaryotic community structure in the Panarea Island hydrothermal system

Our results show that prokaryotic assemblages were mainly shaped by depth and depth-related drivers (Fig. 8), as already found in other shallow Mediterranean systems under summer stratification (e.g., Tinta et al. 2015). Interestingly, prokaryotic assemblages within the two separate layers were very homogenous (horizontally) not only along the transect but also compared to the 'reference' station P0, located 10 km north of the island. However, in our data set, the vent did affect the structure of microbial communities only at their proximity, possibly due to the rapid dispersion of the vent fluids by the hydrodynamic regime.

The water column community was dominated by Proteobacteria and Cyanobacteria (Fig. 7), which are recognized as major players in many marine systems (Cottrell and Kirchman 2000; Rappé et al. 2000; Morris et al. 2002). In particular, the most represented taxa in the upper warmer and low-chlorophyll layer were SAR11 and *Synechococcus*. SAR11 clades are made up of various subgroups with different environmental preferences (Carlson et al. 2009; Morris et al. 2012), living in specific niches. In our study, we found a prevalence of clade Ia over clade II, as often evidenced in coastal systems (Auladell et al. 2022). The high abundance of SAR11 could also be explained by the metabolic effect of proteorhodopsin (light dependent proton pump) that provide an energetic boost in organic-poor environments (Giovannoni et al. 2005). *Synechococcus* is known to thrive in warm surface oligotrophic waters where its accessory pigments (phycoerythrin; Everroad and Wood 2012) provide an adaptive advantage over *Prochlorococcus* whereas its high surface to volume ratio (Moutin et al. 2002) outcompetes phototrophic eukaryotes in nutrient uptake.

Besides a consistent relative contribution of SAR11 (ca. 10%), the lower, cooler and high(er)-chlorophyll layer was dominated by *Prochlorococcus* and genera belonging to the families Flavobacteriaceae (NS2, NS4, NS5, NS9) and Rhodobacteraceae (formerly known as the Roseobacter group). The small cell size of *Prochlorococcus* leads to a high surface-to-volume ratio that facilitates efficient nutrient acquisition and enhances light absorption, which, when combined with its unique pigmentation and broad temperature optima for growth, make it the most efficient light absorber of any photosynthetic cell, thus adapted to subsurface ocean layers (Biller et al. 2015). Both the Flavobacteriaceae and the Rhodobacteraceae are often found in association with high microalgal biomass, being capable of effectively degrading phytoplankton-derived organic matter, spanning from sugars and proteins to low molecular weight compounds such as DMSP and taurine (Moran et al. 2007; Teeling et al. 2012).

Within this 'typical' coastal Mediterranean picture (Auladell et al. 2022), the venting stations were characterized

by high relative abundance of the chemoautotrophic bacterial genus *Thiomicrohabdus* (formerly known as *Thiomicrospira*), specifically where DIC concentration was high (bottom of stations V35 and V23, Fig. 3c). This genus is known to be a culturable sulfide-oxidizer, dominant at shallow hydrothermal vents and extreme environments (Tarasov et al. 2005; Scott et al. 2019). It uses reduced sulfur compounds (e.g., thiosulfate, tetrathionate, sulfur and sulfide) as electron donors and obtains carbon from CO₂ fixation. Cultivation-based studies revealed that sulfur compounds are essential substrates for this bacterium in hydrothermal vent systems (Jannasch et al. 1985). Culture-independent methods revealed that *Thiomicrohabdus* are predominant members in hydrothermal vent communities, such as sulfide chimneys and the Lost City carbonate chimney in the Southwest Indian Ridge (Cao et al. 2014) and the Mid-Atlantic Ridge site (Wirsen et al. 1998) and in extreme environments (Scott et al. 2019). In our study, *Thiomicrohabdus* was dominant in bottom samples of vent-affected stations, in agreement with previous surveys in the Panarea Island area (Manini et al. 2008; Maugeri et al. 2009; Karuza et al. 2012; Lentini et al. 2014) and in other shallow hydrothermal vents in the Mediterranean Sea (Sievert et al. 1999; Patwardhan et al. 2018, 2021). Noteworthy, the relative abundance of *Thiomicrohabdus* decreased with increasing distances from the emission points, suggesting a very rapid dilution effect.

In this natural laboratory, future studies should focus on the benthic-pelagic coupling at the vent sites to unravel the magnitude and the extent of the vent's influence on the C and S cycles. Furthermore, resolving the plume dynamics at a higher spatial resolution would allow to depict the fate of the vent-associated microbiome and its biogeochemical consequences in the oligotrophic Mediterranean. When considering natural laboratories, in order to dissect the effect of atmospheric-driven from hydrothermal-driven acidification on marine microbes and their role in biogeochemical cycles it will be important to compare vents characterized by CO₂ only and by CO₂ + H₂S emissions. These findings could contribute to a better understanding of the role of microbes in the future ocean.

Supplementary Information The online version contains supplementary material available at <https://doi.org/10.1007/s00227-023-04247-8>.

Acknowledgements The project's ship-time was funded by Eurofleets, with work being performed as a sub-project of the Seventh Framework Programme projects "ECO2" and "RISCS", which provided subsidiary funding. The help of the captain and of the crew of the R/V Urania is kindly acknowledged. The authors would like to thank M. Kralj for nutrient analyses, C. Comici for CHN data and A. Karuza for microscopy counts. The comments of two anonymous reviewers helped improving the original version of the manuscript.

Author contributions MC, MG and CDV coordinated the fieldwork. MC, MG, and CDV provided resources. MC, FM, MG, AS, EB, VF, VM and CDV performed data curation, sequencing work and lab work.

AS, EB, VF and VM conducted the bioinformatics analysis. AS, FM and MC wrote the manuscript with the help and inputs from all the authors.

Funding Open access funding provided by Istituto Nazionale di Oceanografia e di Geofisica Sperimentale within the CRUI-CARE Agreement.

Data availability Physical, chemical and microbiological data are freely accessible in Pangea at the following links: <https://doi.pangaea.de/10.1594/PANGAEA.817482>; <https://doi.pangaea.de/10.1594/PANGAEA.804481>; <https://doi.pangaea.de/10.1594/PANGAEA.831927>; <https://doi.pangaea.de/10.1594/PANGAEA.831925>; <https://doi.pangaea.de/10.1594/PANGAEA.831926>. Fastq sequence files are available at the National Center for Biotechnology Information in Sequence Read Archive (SRA) repository (accession number: BioProject PRJNA864835): <https://www.ncbi.nlm.nih.gov/sra/PRJNA864835>.

Declarations

Conflicts of interest The authors declare that the research was conducted in the absence of any commercial or financial relationships that could be construed as a potential conflict of interest.

Ethical approval No ethical approval or permit for animal experimentation was required.

Open Access This article is licensed under a Creative Commons Attribution 4.0 International License, which permits use, sharing, adaptation, distribution and reproduction in any medium or format, as long as you give appropriate credit to the original author(s) and the source, provide a link to the Creative Commons licence, and indicate if changes were made. The images or other third party material in this article are included in the article's Creative Commons licence, unless indicated otherwise in a credit line to the material. If material is not included in the article's Creative Commons licence and your intended use is not permitted by statutory regulation or exceeds the permitted use, you will need to obtain permission directly from the copyright holder. To view a copy of this licence, visit <http://creativecommons.org/licenses/by/4.0/>.

References

- Acosta Pomar ML, Giuffrè G (1996) Pico-, nano- and microplankton communities in hydrothermal marine coastal environments of the Eolian Islands (Panarea and Vulcano) in the Mediterranean Sea. *J Plankton Res* 18:715–730. <https://doi.org/10.1093/plankt/18.8.1519>
- Allgaier M, Riebesell U, Vogt M et al (2008) Coupling of heterotrophic bacteria to phytoplankton bloom development at different pCO₂ levels: a Mesocosm Study. *Biogeosciences* 5:1007–1022. <https://doi.org/10.5194/bg-5-1007-2008>
- Arnosti C (2011) Microbial extracellular enzymes and the marine carbon cycle. *Annu Rev Mar Sci* 3:401–425. <https://doi.org/10.1146/annurev-marine-120709-142731>
- Auladell A, Barberán A, Logares R, Garcés E, Gasol JM, Ferrera I (2022) Seasonal niche differentiation among closely related marine bacteria. *ISME J* 16:178–189. <https://doi.org/10.1038/s41396-021-01053-2>
- Bach LT, Taucher J (2019) CO₂ effects on diatoms: a synthesis of more than a decade of ocean acidification experiments with natural communities. *Ocean Sci* 15:1159–1175. <https://doi.org/10.5194/os-15-1159-2019>

- Bennett SA, Statham PJ, Green DRH et al (2011) Dissolved and particulate organic carbon in hydrothermal plumes from the East Pacific Rise, 9°50'N. *Deep Sea Res I* 58:922–931. <https://doi.org/10.1016/j.dsr.2011.06.010>
- Bergamin L, Bella L, Ferraro L et al (2019) Benthic foraminifera in a coastal marine area of the eastern Ligurian Sea (Italy): response to environmental stress. *Ecol Indic* 96:16–31. <https://doi.org/10.1016/j.ecolind.2018.08.050>
- Biller SJ, Berube PM, Lindell D, Chisholm SW (2015) *Prochlorococcus*: the structure and function of collective diversity. *Nat Rev Microbiol* 13:13–27. <https://doi.org/10.1038/nrmicro3378>
- Bokulich NA, Dillon MR, Zhang Y et al (2018) q2-longitudinal: longitudinal and paired-sample analyses of microbiome data. *mSystems* 3:e00219–18. <https://doi.org/10.1128/mSystems.00219-18>
- Bolyen E, Rideout JR, Dillon MR (2019) Reproducible, interactive, scalable and extensible microbiome data science using QIIME 2. *Nat Biotechnol* 37:852–857. <https://doi.org/10.1038/s41587-019-0209-9>
- Bortoluzzi G, Romeo T, La Cono V, La Spada G, Smedile F, Esposito V, Sabatino G, Di Bella M, Canese S, Scotti G, Bo M, Giuliano L, Jones D, Golyshin PN, Yakimov MM, Andaloro F (2017) Ferrous iron- and ammonium-rich diffuse vents support habitat-specific communities in a shallow hydrothermal field off the Basiluzzo Islet (Aeolian Volcanic Archipelago). *Geobiology* 15:664–677. <https://doi.org/10.1111/gbi.12237>
- Boyd PW, Collins S, Dupont S, Fabricius K, Gattuso J-P, Havenhand J et al (2018) Experimental strategies to assess the biological ramifications of multiple drivers of global ocean change—a review. *Glob Change Biol* 24:2239–2261. <https://doi.org/10.1111/gcb.14102>
- Caliro S, Caracausi A, Chiodini G et al (2004) Evidence of a recent input of magmatic gases into the quiescent volcanic edifice of Panarea, Aeolian Islands, Italy. *Geophys Res Lett* 31:L07619. <https://doi.org/10.1029/2003GL019359>
- Callahan BJ, McMurdie PJ, Rosen MJ et al (2016) DADA2: high-resolution sample inference from illumina amplicon data. *Nat Methods* 13(581–583):544. <https://doi.org/10.1038/nmeth.3869>
- Cao H, Wang Y, Lee OO et al (2014) Microbial sulfur cycle in two hydrothermal chimneys on the southwest Indian ridge. *mBio* 5:e00980–13. <https://doi.org/10.1128/mBio.00980-13>
- Carlson CA, Morris R, Parsons R et al (2009) Seasonal dynamics of SAR11 populations in the euphotic and mesopelagic zones of the northwestern Sargasso Sea. *ISME J* 3:283–295. <https://doi.org/10.1038/ismej.2008.117>
- Celussi M, Malfatti F, Franzo A et al (2017) Ocean acidification effect on prokaryotic metabolism tested in two diverse trophic regimes in the Mediterranean Sea. *Estuar Coast Shelf Sci* 186:125–138. <https://doi.org/10.1016/j.ecss.2015.08.015>
- Coffin RB, Montgomery MT, Boyd TJ, Masutani SM (2004) Influence of ocean CO₂ sequestration on bacterial production. *Energy* 29:1511–1520. <https://doi.org/10.1016/j.energy.2003.06.001>
- Cottrell MT, Kirchman DL (2000) Community composition of marine bacterioplankton determined by 16S rDNA clone libraries and fluorescence in situ hybridization. *Appl Environ Microbiol* 66:5116–5122. <https://doi.org/10.1128/AEM.66.12.5116-5122.2000>
- Dickson AG, Sabine CL, Christian J (2007) Guide to best practices for ocean CO₂ measurements. *PICES Spec Publ* 3:191
- Dittmar T, Koch BP (2006) Thermogenic organic matter dissolved in the abyssal ocean. *Mar Chem* 102:208–217. <https://doi.org/10.1016/j.marchem.2006.04.003>
- Esposito A, Giordano G, Anzidei M (2006) The 2002–2003 submarine gas eruption at Panarea volcano (Aeolian Islands, Italy): volcanology of the seafloor and implications for the hazard scenario. *Mar Geol* 227:119–134. <https://doi.org/10.1016/j.margeo.2005.11.007>
- Everroad RC, Wood AM (2012) Phycoerythrin evolution and diversification of spectral phenotype in *Synechococcus* and related cyanobacteria. *Mol Phylogenet Evol* 64:381–392. <https://doi.org/10.1016/j.ympev.2012.04.013>
- Flynn KJ, Clark DR, Mitra A, Fabian H, Hansen PJ, Gilbert PM, Wheeler GL, Stoecker DK, Blackford JC, Brownlee C (2015) Ocean acidification with (de)eutrophication will alter future phytoplankton growth and succession. *Proc R Soc B* 282:20142604. <https://doi.org/10.1098/rspb.2014.2604>
- Fukuda R, Sohrin Y, Saotome N et al (2000) Koike East-west gradient in ectoenzyme activities in the subarctic Pacific: possible regulation by zinc. *Limnol Oceanogr* 45:930–939. <https://doi.org/10.4319/lo.2000.45.4.0930>
- Giovannoni S, Bibbs L, Cho JC et al (2005) Proteorhodopsin in the ubiquitous marine bacterium SAR11. *Nature* 438:82–85. <https://doi.org/10.1038/nature04032>
- Gomez-Saez GV, Niggemann J, Dittmar T et al (2016) Molecular evidence for abiotic sulfurization of dissolved organic matter in marine shallow hydrothermal systems. *Geochim Cosmochim Acta* 190:35–52. <https://doi.org/10.1016/j.gca.2016.06.027>
- González-Delgado A, Hernández JC (2018) Chapter two—the importance of natural acidified systems in the study of ocean acidification: what have we learned? *Adv Mar Biol* 80:57–99. <https://doi.org/10.1016/bs.amb.2018.08.001>
- González FJ, Rincón-Tomás B, Somoza L, Santofimia E, Medialdea T et al (2020) Low-temperature, shallow-water hydrothermal vent mineralization following the recent submarine eruption of Tagoro volcano (El Hierro, Canary Islands). *Mar Geol* 430: 106333. <https://doi.org/10.1016/j.margeo.2020.106333>
- Gottschalk G (1979) Nutrition of bacteria. In: *Bacterial metabolism*. Springer, New York, NY. p. 1–11. https://doi.org/10.1007/978-1-4684-0465-4_1
- Grossart H-P, Allgaier M, Passow U, Riebesell U (2006) Testing the effect of CO₂ concentration on the dynamics of marine heterotrophic bacterioplankton. *Limnol Oceanogr* 51:1–11. <https://doi.org/10.4319/lo.2006.51.1.0001>
- Gugliandolo C, Maugeri TL (2019) Phylogenetic diversity of archaea in shallow hydrothermal vents of Eolian Islands, Italy. *Diversity* 11:156. <https://doi.org/10.3390/d11090156>
- Hoppe HG (1993) Use of fluorogenic model substrates for extracellular enzyme activity (EEA) measurement of bacteria. In: Kemp PF, Sherr BF, Sherr EB, Cole JJ (eds) *Handbook of methods in aquatic microbial ecology*. CRC Press, Boca Raton, pp 423–431
- Hu C, Li X, He M, Jiang P, Long A, Xu J (2021) Effect of ocean acidification on bacterial metabolic activity and community composition in oligotrophic oceans, inferred from short-term bioassays. *Front Microbiol* 12: 583982. <https://doi.org/10.3389/fmicb.2021.583982>
- Hutchins DA, Fu FX, Zhang Y et al (2007) CO₂ control of *Trichodesmium* N₂ fixation, photosynthesis, growth rates, and elemental ratios: implications for past, present, and future ocean biogeochemistry. *Limnol Oceanogr* 52:1293–1304. <https://doi.org/10.4319/lo.2007.52.4.1293>
- Illumina (2013) 16S metagenomic sequencing library preparation. https://www.illumina.com/content/dam/illumina-support/documents/documentation/chemistry_documentation/16s/16s-metagenomic-library-prep-guide-15044223-b.pdf
- Italiano F, Nuccio P (1991) Geochemical investigations of submarine volcanic exhalations to the east of Panarea, Aeolian Islands, Italy. *J Volcanol Geotherm Res* 46:125–141. [https://doi.org/10.1016/0377-0273\(91\)90079-f](https://doi.org/10.1016/0377-0273(91)90079-f)
- Jacobson Meyers ME, Sylvan JB, Edwards KJ (2014) Extracellular enzyme activity and microbial diversity measured on seafloor exposed basalts from Loihi seamount indicate the importance of basalts to global biogeochemical cycling. *Appl Environ Microbiol* 80:4854–4864. <https://doi.org/10.1128/AEM.01038-14>
- Jannasch HW, Wirsén CO, Nelson DC, Robertson LA (1985) *Thiomicrospira crunigena* sp. nov., a colorless, sulfur-oxidizing

- bacterium from a deep-sea hydrothermal vent. *Int J Syst Evol Microbiol* 35:422–424. <https://doi.org/10.1099/00207713-35-4-422>
- Jones DG, Beaubien SE, Blackford JC, Foekema EM, Lions J, De Vitor C, West JM, Widdicombe S, Hauton C, Queirós AM (2015) Developments since 2005 in understanding potential environmental impacts of CO₂ leakage from geological storage. *Int J Greenh Gas Control* 40:350–377. <https://doi.org/10.1016/j.ijggc.2015.05.032>
- Karl DM (1995) Ecology of free-living, hydrothermal vent microbial communities. In: Karl DM (ed) *The microbiology of deep-sea hydrothermal vents*. CRC Press Inc, Boca Raton, pp 35–126
- Karuza A, Celussi M, Cibic T et al (2012) Virioplankton and bacterioplankton in a shallow CO₂-dominated hydrothermal vent (Panarea Island, Tyrrhenian Sea). *Estuar Coast Shelf Sci* 97: 10–18. <https://doi.org/10.1016/j.ecss.2011.10.027>
- Kirchman D, K'nees E, Hodson R (1985) Leucine incorporation and its potential as a measure of protein synthesis by bacteria in natural aquatic systems. *Appl Environ Microbiol* 49: 599–607. <https://doi.org/10.1128/aem.49.3.599-607.1985>
- Koroleff F, Grasshof K (1983) Determination of nutrients. In: Grasshof K, Erhardt M, Kremling K (eds) *Methods of seawater analyses 2*. Verlag Chemie, p 125–188
- Lang SQ, Butterfield DA, Lilley MD et al (2006) Dissolved organic carbon in ridge-axis and ridge-flank hydrothermal systems. *Geochim Cosmochim Acta* 70:3830–3842. <https://doi.org/10.1016/j.gca.2006.04.031>
- Le S, Josse J, Husson F (2008) FactoMineR: an R package for multivariate analysis. *J Stat Softw* 25: 1–18. <https://doi.org/10.18637/jss.v025.i01>
- Lentini V, Gugliandolo C, Boyke B, Jorg O, Maugeri T (2014) Diversity of prokaryotic community at a shallow marine hydrothermal site elucidated by Illumina sequencing technology. *Curr Microbiol* 69: 457–466. <https://doi.org/10.1007/s00284-014-0609-5>
- Lidbury I, Johnson V, Hall-Spencer JM, Munn CB, Cunliffe M (2012) Community-level response of coastal microbial biofilms to ocean acidification in a natural carbon dioxide vent ecosystem. *Mar Pollut Bull* 64:1063–1066. <https://doi.org/10.1016/j.marpolbul.2012.02.011>
- Liu J, Weinbauer MG, Maier C, Dai M, Gattuso J-P (2010) Effect of ocean acidification on microbial diversity and microbe-driven biogeochemistry and ecosystem functioning. *Aquat Microb Ecol* 61: 291–305. <https://doi.org/10.3354/ame01446>
- Longhurst AR, Harrison WG (1989) The biological pump: profiles of plankton production and consumption in the upper ocean. *Prog Oceanogr* 22:47–123. [https://doi.org/10.1016/0079-6611\(89\)90010-4](https://doi.org/10.1016/0079-6611(89)90010-4)
- Lorenzen CJ, Jeffrey SW (1980) Determination of chlorophyll in seawater. *UNESCO Tech Pap Mar Sci* 35:1–20
- Lorrain A, Savoye N, Chauvaud L et al (2003) Decarbonation and preservation method for the analysis of organic c and n contents and stable isotope ratios of low carbonated suspended particulate material. *Anal Chim Acta* 491:125–133. [https://doi.org/10.1016/S0003-2670\(03\)00815-8](https://doi.org/10.1016/S0003-2670(03)00815-8)
- Macias D, Garcia-Gorrioz E, Stips A, Huertas IE (2019) Non-redfieldian dynamics driven by phytoplankton phosphate frugality explain nutrient and chlorophyll patterns in model simulations for the Mediterranean Sea. *Prog Oceanogr* 173:37–50. <https://doi.org/10.1016/j.pocean.2019.02.005>
- Manini E, Luna GM, Corinaldesi C, Zeppilli D, Bortoluzzi G, Caramanna G, Raffa F, Danovaro R (2008) Prokaryote diversity and virus abundance in shallow hydrothermal vents of the Mediterranean Sea (Panarea Island) and the Pacific Ocean (north Sulawesi-Indonesia). *Microb Ecol* 55:626–639. <https://doi.org/10.1007/s00248-007-9306-2>
- Maugeri TL, Lentini V, Gugliandolo C et al (2009) Bacterial and archaeal populations at two shallow hydrothermal vents off Panarea Island (Eolian Islands, Italy). *Extremophiles* 13:199–212. <https://doi.org/10.1007/s00792-008-0210-6>
- Maugeri TL, Bianconi G, Canganella F et al (2010) Shallow hydrothermal vents in the southern Tyrrhenian sea. *Chem Ecol* 26:285–298. <https://doi.org/10.1080/02757541003693250>
- McMurdie PJ, Holmes S (2012) Phyloseq: a bioconductor package for handling and analysis of high-throughput phylogenetic sequence data. *Pac Symp Biocomput* 235–46
- Molari M, Guilini K, Lott C et al (2018) CO₂ leakage alters biogeochemical and ecological functions of submarine sands. *Sci Adv* 4: eaao2040. <https://doi.org/10.1126/sciadv.aao2040>
- Moran MA, Belas R, Schell MA, González JM, Sun F, Sun S, Binder BJ, Edmonds J, Ye W, Orcutt B, Howard EC, Meile C, Palefsky W, Goesmann A, Ren Q, Paulsen I, Ulrich LE, Thompson LS, Saunders E, Buchan A (2007) Ecological genomics of Roseobacters. *Appl Environ Microbiol* 73:14. <https://doi.org/10.1128/AEM.02580-06>
- Morris RM, Rappé MS, Connon SA et al (2002) SAR11 clade dominates ocean surface bacterioplankton communities. *Nature* 420:806–810. <https://doi.org/10.1038/nature01240>
- Morris RM, Frazer C, Carlson CA (2012) Basin-scale patterns in the abundance of SAR11 subclades, marine Actinobacteria (OM1), members of the Roseobacter clade and OCS116 in the South Atlantic. *Environ Microbiol* 14:1133–1144
- Moutin T, Thingstad TF, Van Wambecke F, Marie D, Slawyk G, Rimbault P, Claustre H (2002) Does competition for nanomolar phosphate supply explain the predominance of the cyanobacterium *Synechococcus*? *Limnol Oceanogr* 47: 1562–1567. <https://doi.org/10.4319/lo.2002.47.5.1562>
- Noble R, Fuhrman J (1998) Use of SYBR green I for rapid epifluorescence counts of marine viruses and bacteria. *Aquat Microb Ecol* 14:113–118. <https://doi.org/10.3354/ame014113>
- Oksanen J, Blanchet FG, Friendly M et al (2019) Vegan: community ecology package. R Package Version 2:5–6
- Parada AE, Needham DM, Fuhrman JA (2016) Every base matter: assessing small subunit rRNA primers for marine microbiomes with mock communities, time series and global field samples. *Environ Microbiol* 18:1403–1414. <https://doi.org/10.1111/1462-2920.13023>
- Patel A, Noble RT, Steele JA et al (2007) Virus and prokaryote enumeration from planktonic aquatic environments by epifluorescence microscopy with SYBR green I. *Nat Protoc* 2:269–276. <https://doi.org/10.1038/nprot.2007.6>
- Patwardhan S, Foustoukos DI, Giovannelli D, Yucel M, Vetriani C (2018) Ecological succession of sulfur-oxidizing epsilon- and gammaproteobacteria during colonization of a shallow-water hydrothermal vent. *Front Microbiol* 9: 2970. <https://doi.org/10.3389/fmicb.2018.02970>
- Patwardhan S, Smedile F, Giovannelli D, Vetriani C (2021) Metagenomic profiling of chemosynthetic microbial biofilms reveal metabolic flexibility during colonization of shallow-water gas vent. *Front Microbiol* 12: 638300. <https://doi.org/10.3389/fmicb.2021.638300>
- Pella E, Colombo B (1973) Study of carbon, hydrogen and nitrogen determination by combustion-gas chromatography. *Microchim Acta* 61:697–719. <https://doi.org/10.1007/BF01218130>
- Piontek J, Lunau M, Händel CB et al (2010) Engel acidification increases polysaccharide degradation in the ocean. *Biogeosciences* 7:1615–1624
- Piontek J, Borchard C, Sperling M et al (2013) Engel response of bacterioplankton activity in an Arctic fjord system to elevated pCO₂: results from a mesocosm perturbation study. *Biogeosciences* 10: 297–314

- Pomeroy LR, Wiebe WJ (2001) Temperature and substrate as interactive limiting factors for marine heterotrophic bacteria. *Aquat Microb Ecol* 23:187–204
- Quast C, Pruesse E, Yilmaz P, Gerken J, Schweer T, Yarza P et al (2013) The SILVA ribosomal RNA gene database project: improved data processing and web-based tools. *Nucleic Acids Res* 41:590–596. <https://doi.org/10.1093/nar/gks1219>
- R Core Team (2019) R: a language and environment for statistical computing [Computer software R Foundation for Statistical Computing]. R Core Team, Vienna
- Rappé MS, Vergin K, Giovannoni SJ (2000) Phylogenetic comparisons of a coastal bacterioplankton community with its counterparts in open ocean and freshwater systems. *FEMS Microbiol Ecol* 33:219–232. <https://doi.org/10.1111/j.1574-6941.2000.tb00744.x>
- Riebesell U, Gattuso J-P (2015) Lessons learned from ocean acidification research. *Nat Clim Change* 5: 12–14. <https://doi.org/10.1038/nclimate2456>
- Rizzo C, Arcadi E, Calogero R, Scutтери V et al (2022) Ecological and biotechnological relevance of mediterranean hydrothermal vent systems. *Minerals* 12:251. <https://doi.org/10.3390/min12020251>
- Sala MM, Aparicio FL, Balague V, Boras JA, Borrull E, Cardelus C, Cros L, Gomes A, Lopez-Sanz A, Malits A et al (2016) Contrasting effects of ocean acidification on the microbial food web under different trophic conditions. *ICES J Mar Sci* 73:670–679. <https://doi.org/10.1093/icesjms/fsv130>
- Schlitzer R (2018) Ocean data view. <https://odv.awi.de>
- Scutтери V, Smedile F, Vizzini S, Mazzola A, Vetriani C (2022) Microbial biofilms along a geochemical gradient at the shallow-water hydrothermal system of Vulcano Island, Mediterranean Sea. *Front Microbiol* 13: 840205. <https://doi.org/10.3389/fmicb.2022.840205>
- Scott KM, Leonard JM, Boden R et al (2019) Diversity in CO₂-concentrating mechanisms among *Chemolithoautotrophs* from the genera *Hydrogenovibrio*, *Thiomicrospira*, and *Thiomicrospira*, ubiquitous in sulfidic habitats worldwide. *Appl Environ Microbiol* 85:2096–2118. <https://doi.org/10.1128/AEM.02096-18>
- Sharp JH (1974) Improved analysis for “particulate” organic carbon and nitrogen from seawater. *Limnol Oceanogr* 19:984–989. <https://doi.org/10.4319/lo.1974.19.6.0984>
- Sievert SM, Brinkhoff T, Muyzer G, Ziebis W, Kuever J (1999) Spatial heterogeneity of bacterial populations along an environmental gradient at a shallow submarine vent near Milos Island (Greece). *Appl Environ Microbiol* 65:3834–3842. <https://doi.org/10.1128/AEM.65.9.3834-3842.1999>
- Simon M, Azam F (1989) Protein content and protein synthesis rates of planktonic marine bacteria. *Mar Ecol Prog Ser* 51:201–213. <https://doi.org/10.3354/meps051201>
- Smith DC, Azam F (1992) A simple, economical method for measuring bacterial protein synthesis rates in seawater using 3H-leucine. *Mar Microb Food Webs* 6:107–114
- Tangherlini M, Corinaldesi C, Ape F, Greco S, Romeo T, Anladolo F, Danovaro R (2021) Ocean acidification induces changes in virus-host relationship in Mediterranean benthic ecosystems. *Microorganisms* 9:769. <https://doi.org/10.3390/microorganisms9040769>
- Tarasov V, Gebruk A, Mironov A, Moskalev L (2005) Deep-sea and shallow-water hydrothermal vent communities: two different phenomena? *Chem Geol* 224:5–39. <https://doi.org/10.1016/j.chemgeo.2005.07.021>
- Taucher J, Boxhammer T, Bach LT, Paul AJ, Schartau M, Stange P, Riebesell U (2021) Changing carbon-to-nitrogen ratios of organic-matter export under ocean acidification. *Nat Clim Chang* 11:52–57. <https://doi.org/10.1038/s41558-020-00915-5>
- Teeling H, Fuchs BM, Becher D, Klockow C, Gardebrecht A, Bennek CM, Kassabgy M et al (2012) Substrate-controlled succession of marine bacterioplankton populations induced by a phytoplankton bloom. *Science* 336: 608–611. <https://doi.org/10.1126/science.1218344>
- Tinta T, Vojvoda J, Mozetič P, Talaber I, Vodopivec M, Malfatti F, Turk V (2015) Bacterial community shift is induced by dynamic environmental parameters in a changing coastal ecosystem (northern Adriatic, northeastern Mediterranean Sea)—a 2-year time-series study. *Environ Microbiol* 17:3581–3596. <https://doi.org/10.1111/1462-2920.12519>
- Tsiola A, Krasakopoulou E, Daffonchio D, Frangoulis C, Tzagaraki TM, Fodelianakis S, Pitta P (2023) Responses of free-living planktonic bacterial communities to experimental acidification and warming. *Microorganisms* 11:273. <https://doi.org/10.3390/microorganisms11020273>
- Walker BD, Mccarthy MD, Fisher AT, Guilderson TP (2008) inorganic carbon isotopic composition of low-temperature axial and ridge-flank hydrothermal fluids of the Juan de Fuca Ridge. *Mar Chem* 108:123–136
- Waterbury JB, Watson SW, Guillard RRL, Brand LE (1979) Widespread occurrence of a unicellular, marine, planktonic, cyanobacterium. *Nature* 227:293–294. <https://doi.org/10.1038/277293a0>
- Wickham H (2016) ggplot2. Springer Cham, p 260
- Wirsen CO, Brinkhoff T, Kuever J et al (1998) Comparison of a new *Thiomicrospira* strain from the mid-Atlantic ridge with known hydrothermal vent isolates. *Appl Environ Microbiol* 64: 4057–4059. <https://doi.org/10.1128/AEM.64.10.4057-4059.1998>
- Yamada N, Suzumura M (2010) Effects of seawater acidification on hydrolytic enzyme activities. *J Oceanogr* 66:233–241. <https://doi.org/10.1007/s10872-010-0021-0>
- Zuur AF, Ieno EN, Elphick CS (2010) A protocol for data exploration to avoid common statistical problems. *Methods Ecol Evol* 1:3–14. <https://doi.org/10.1111/j.2041-210X.2009.00001.x>

Publisher's Note Springer Nature remains neutral with regard to jurisdictional claims in published maps and institutional affiliations.